

# Design of a hydrogen filled Cedar



NA62 INTERNAL NOTE  
NA62-2021-03

Jack Henshaw <sup>†</sup> & John Fry <sup>††</sup>

University of Birmingham

25/01/2021

---

## Abstract

To ensure the necessary precision for the  $K^+ \rightarrow \pi^+ \nu\bar{\nu}$  analysis, KTAG is required to have a time resolution less than 100ps, greater than 95% kaon identification efficiency, and a pion misidentification probability of less than  $10^{-4}$ . Based on Cedar-W filled with nitrogen as the Cherenkov radiator, KTAG has more than fulfilled these performance requirements. In order to reduce the multiple scattering of beam particles in the gas, it is desirable to replace the nitrogen by hydrogen whilst maintaining current performance. This report explains the changes to the Cedar optics necessary to do this and presents a design for a hydrogen pressure of 3.80 bar, together with a discussion of the optical and mechanical tolerances required to build it.

---

<sup>†</sup>Email: jack.henshaw@cern.ch

<sup>††</sup>Email: jrf@liverpool.ac.uk

# Contents

|          |  |           |
|----------|--|-----------|
| <b>1</b> | <b>Introduction</b>                                    | <b>2</b>  |
| <b>2</b> | <b>Redesign of KTAG</b>                                | <b>4</b>  |
| 2.1      | Design Methodology for Cedar-H . . . . .               | 4         |
| 2.2      | Further KTAG Optical Considerations . . . . .          | 5         |
| 2.3      | Performance of KTAG . . . . .                          | 6         |
| <b>3</b> | <b>Proposed KTAG with Cedar-H at 3.8 bar</b>           | <b>7</b>  |
| <b>4</b> | <b>Tolerances on Optical and Mechanical Parameters</b> | <b>10</b> |
| <b>5</b> | <b>Summary</b>   | <b>11</b> |
|          | <b>Appendix: Cedar Parameter Values</b>                | <b>12</b> |
|          | <b>Appendix: Tolerance Plots</b>                       | <b>13</b> |

# 1 Introduction

Measurement of the branching fraction of the  $K^+ \rightarrow \pi^+ \nu \bar{\nu}$  decay relies on the identification and removal of background originating from the dominant kaon decays, together with various upstream sources arising from interactions of the beam and decay particles with material in the beamline and sub-detectors. Although no evidence has been seen from the analysis of data recorded up to the end of 2018 of any background arising from the nitrogen gas in Cedar-W, it is quite possible that some background may emerge in the future as the experimental sensitivity is increased. As such, it makes sense to investigate whether KTAG can be redesigned to use hydrogen as the Cherenkov radiator, with a significant reduction in the multiple scattering of beam particles in the gas, so that such a detector could be available when needed. For the same Cherenkov angle as for nitrogen the hydrogen pressure would be 3.65 bar compared with 1.71 bar for nitrogen, but even with the somewhat thicker vacuum windows at the higher pressure the amount of material presented to the beam would reduce from  $3.7\%X_0$  to  $0.7\%X_0$  [1].

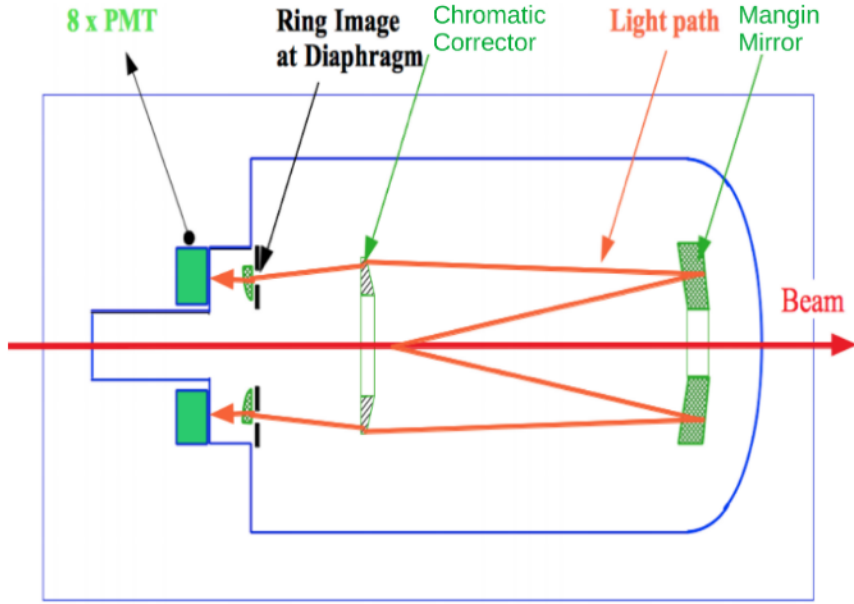


Figure 1: Schematic of a standard Cedar, showing the typical path taken by photons [1]. The eight photomultipliers (PMTs) have since been replaced to meet the high intensity environment of NA62.

Cedar-W [2] is a differential, ring-imaging Cherenkov detector that identifies kaons in the unseparated hadron beam using nitrogen as the Cherenkov radiator. The radiated light is reflected off a Mangin Mirror before being refracted through the Chromatic Corrector, Fig 1. The optical design and gas pressure are such that light radiated by kaons passes through the diaphragm aperture, while light from other particles is absorbed. After the diaphragm the light passes through a set of eight condenser lenses that focus the light through the quartz windows and optical caps. The light is then reflected radially outwards by spherical mirrors and channelled through light guides onto a photomultiplier (PMT) array, as shown in Fig 2.

Because the optics of Cedar-W have been optimised for nitrogen, which has different dispersive behaviour from hydrogen, it is not possible merely to replace the gas in Cedar-W without further change. As can be seen from Fig 3, the wavelength dependence of the radial position of Cherenkov photons reaching the diaphragm of Cedar-W for hydrogen and nitrogen are very different, with considerable overlap in radial position for photons from kaons and pions in the case of hydrogen. In order to prevent Cherenkov photons from pions passing through the diaphragm, a significant fraction of the photons from kaons would be lost and this would seriously compromise the performance of KTAG. Hence a new design, referred to in what follows as Cedar-H, is required.

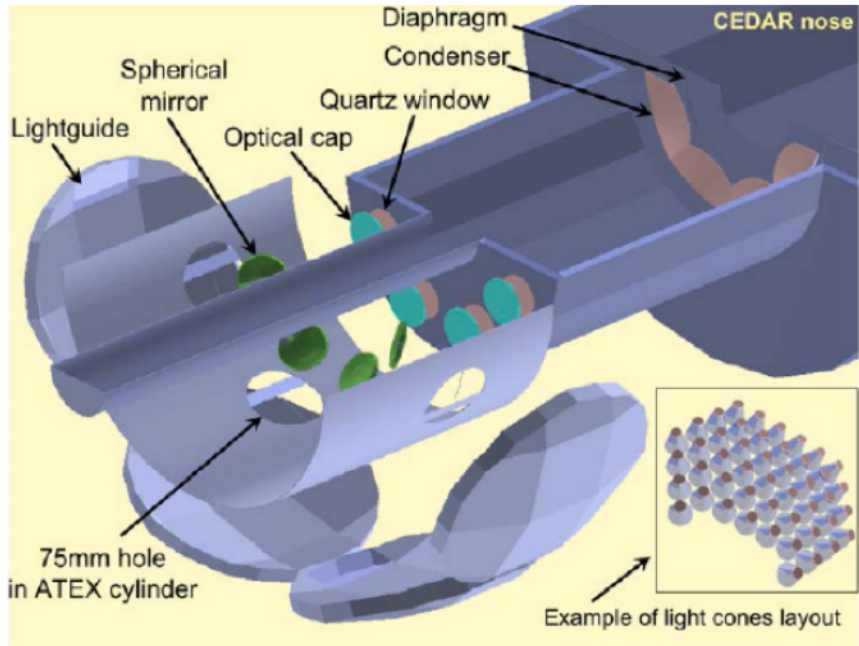


Figure 2: Geant4 visualisation of the KTAG optics replacing the 8 PMTs as shown in Fig 1. Here light travels from right to left before being reflected radially outwards by the spherical mirrors towards the lightguides.

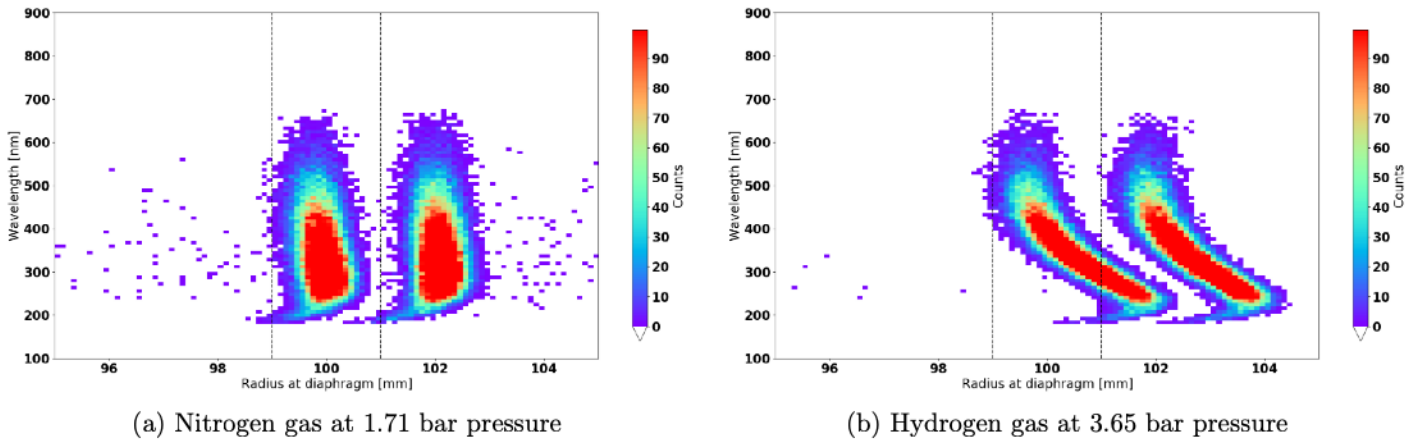


Figure 3: Photon radius at the diaphragm versus wavelength for nitrogen (left) and hydrogen (right) for the current Cedar-W. The kaon (pion) light distribution is on the left (right) with the diaphragm aperture shown by dashed lines. The counts are weighted by the quantum efficiency of the PMTs for the simulation of 1000 kaons and 1000 pions.

## 2 Redesign of KTAG

The redesign of KTAG falls naturally into two parts: first the number of Cherenkov photons (weighted by the quantum efficiency of the photodetectors) passing through the narrow Cedar diaphragm aperture must be maximised; secondly, this Cherenkov light must be transformed by the optics external to Cedar-H into a pattern that fully illuminates the photodetector arrays. We aim to find a design that produces at least 10% more photoelectrons per kaon than is currently achieved with the nitrogen radiator, and for safety reasons the hydrogen pressure in Cedar-H should be as low as can be reasonably achieved. A discussion of the current Cedar-W performances can be found in Ref [3].

### 2.1 Design Methodology for Cedar-H

The new design is based on an existing Cedar-N, which has an identical body and mechanical layout to a Cedar-W. This means, for example, that either of the two rather complex condenser lenses can be used for Cedar-H, the choice of which helps in simplifying the optics external to the Cedar. The mechanical fixtures, rigidly fixed on the inside of the Cedar body, that hold and align the Mangin Mirror and Corrector Lens, Fig 1, are both complex and sophisticated and it was agreed with CERN engineers that no changes would be made to them. This means that the positions and maximum radii of the Mangin Mirror and Corrector Lens are fixed. The parameters to be modified were the two radii of the Mangin Mirror, the radius of the convex surface of the plano-convex Corrector Lens, and the size of the central aperture in the Mangin Mirror that allows beam particles to pass through.

The optical design aims to achieve as good a focus as possible of Cherenkov light at the diaphragm aperture by minimising the defocussing contributions from geometrical aberrations and chromatic dispersion in the quartz and hydrogen media. The principal task of the Mangin Mirror is to reduce aberrations, which is done by varying the ratio of the radii of the mirror and lens surfaces [4], while the Corrector Lens reduces the effects of dispersion, which depend on the ratio of the focal lengths of the Mangin Mirror and Corrector Lenses. The balance between geometrical aberrations and chromatic dispersion changes with gas pressure, and this results in solutions for the optimal radii of the three surfaces that are specific to the particular gas pressure.

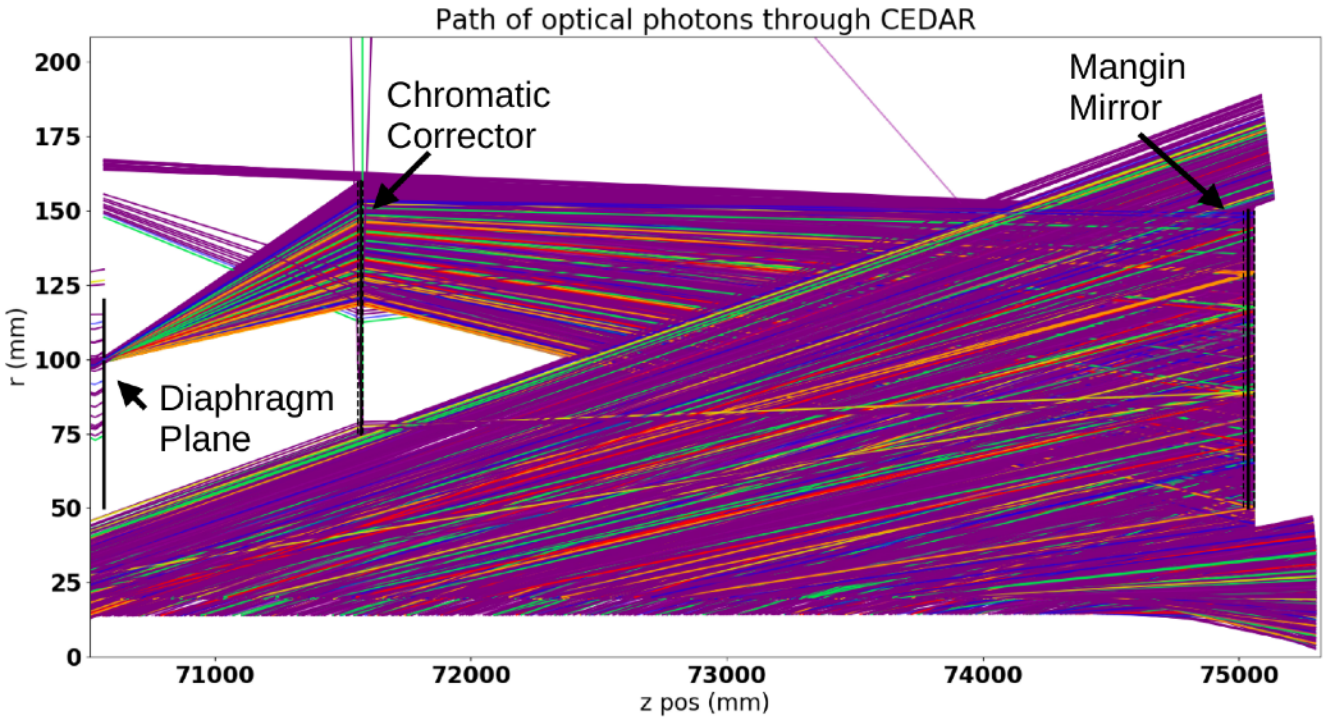


Figure 4: Ray tracing through the Cedar-H internal optics. Cherenkov photons emitted by kaons are traced from the beam (bottom) to the Mangin Mirror (right), they are reflected back towards the Chromatic Corrector and refracted onto the diaphragm plane.

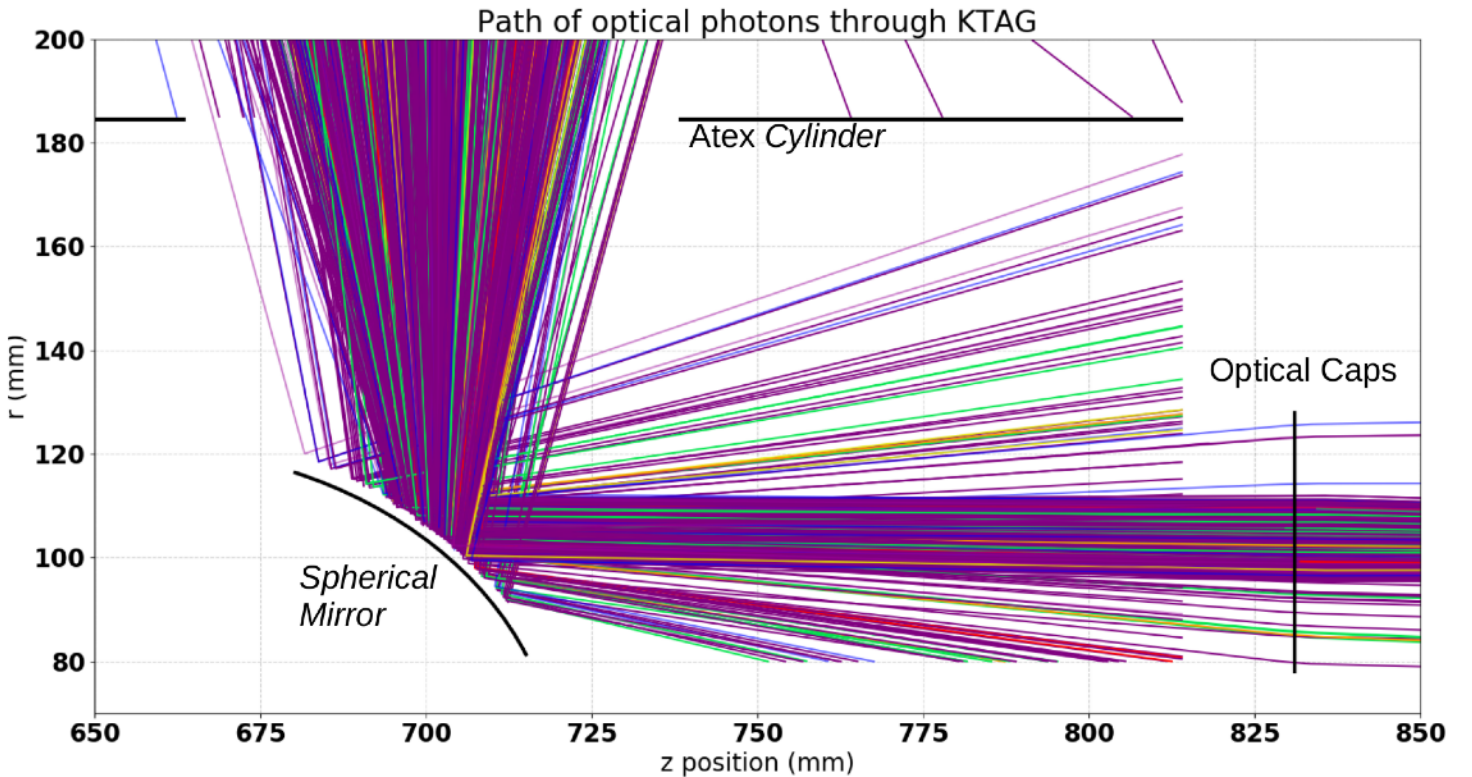


Figure 5: Ray tracing through the Cedar-H external optics. Photons exiting the diaphragm are focused by 8 condenser lenses onto 8 Quartz Windows and then reflected radially outwards by 8 spherical mirrors onto the PMT arrays.

Trial solutions for the optical parameters at a variety of fixed pressures were found by an analytical ray-tracing procedure in two dimensions that made use of the cylindrical symmetry of the Cedar optics. The parameters varied were the ratio of the radii of curvature of the surfaces of the Mangin Mirror, and the focal lengths of the Mangin Mirror and the Corrector Lens. An iterative approach was used to minimise the width of the reflected light spot at the diaphragm aperture, with successful solutions required to have an RMS spot size smaller than 0.5mm. A refinement of these solutions used NA62MC enabling Cherenkov light to be generated in three dimensions over a broader range of wavelengths and points of origin, and directly varied the three radii of curvature in an iterative approach. This more powerful tool enabled the light rays to be traced upstream of the Cedar and through the external optics to the photodetectors, Fig 4 and 5. A significant increase in the light focused onto the diaphragm aperture was achieved by reducing the size of the central hole in the Mangin Mirror, while ensuring that the particle beam could pass through safely.

## 2.2 Further KTAG Optical Considerations

When optimising the KTAG optics upstream of Cedar-H there were two requirements: first that the light was correctly directed towards the PMTs, and secondly that the light spot formed was of an appropriate size and shape. It was found that the Condenser lens from Cedar-W, rather than that from Cedar-N, was the better starting point, since the further changes required to the optics were minimal. These involved replacing the eight spherical mirrors that directed light onto the PMT arrays with a minor adjustment to their radial position; it is also possible to change the lenses immediately outside the eight quartz windows but this was found to be unnecessary. As an aside we note that spherical mirrors formed from lenses having a surface with radius of curvature available from an optical catalogue are perfectly satisfactory; no significant gain was achieved when customising the radius of curvature.

### 2.3 Performance of KTAG

In table 1 we show the performance of the redesigned KTAG for five Cedar-H hydrogen pressures varying from 3.7 to 4.1 bar, compared with the performance of Cedar-W filled with nitrogen. The comparison is made using the identical NA62MC framework, where Cedar-W is optically and mechanically unchanged from the detector in situ. We note that the predicted (average) number of photoelectrons detected per kaon is approximately 20% higher for Cedar-W than is measured in the experiment and assume this to be true also for Cedar-H.

From table 1 it can be seen that the Gaussian width of the kaon ring decreases with pressure, while the light yield at the diaphragm increases, as more Cherenkov photons are emitted. This might suggest that the performance of KTAG would be superior at higher pressures. However, this is not the case for two reasons. First, the width of the kaon ring is small compared with the aperture of the diaphragm and all light is collected, so that a decrease in ring width does not bring an added benefit. Secondly, as the pressure increases so does the Cherenkov angle and the size of the spot at the PMT array. Thus, we see a roughly constant number of photoelectrons detected as the pressure increases. Finally, we note from table 1 that both the kaon identification efficiencies and pion misidentification probabilities more than meet the requirements set out in the NA62 design specification [1] at all pressures, and indeed the predicted average number of detected photoelectrons per kaon is approximately 30% higher for Cedar-H than for Cedar-W.

| Pressure<br>[bar]                  | Gaussian<br>Width of<br>Kaon Ring<br>[mm] | Number of<br>Photons At<br>Diaphragm<br>Per Kaon | Number Of<br>Photons At<br>PMTs Per<br>Kaon | Number Of<br>Photons At<br>PMTs Per<br>Pion | Kaon Iden-<br>tification<br>Efficiency | Pion<br>Misidentifi-<br>cation<br>Probability |
|------------------------------------|---|--|---|---|--|---|
| 3.70                               | 0.43                                      | 37.3   | 32.1  | 0.09  | 99.2%                                  | $\lesssim 10^{-4}$                            |
| 3.80                               | 0.36                                      | 38.1   | 32.3  | 0.11  | 99.5%                                  | $\lesssim 10^{-4}$                            |
| 3.90                               | 0.38                                      | 38.8   | 32.8  | 0.10  | 99.5%                                  | $\lesssim 10^{-4}$                            |
| 4.00                               | 0.33                                      | 39.3   | 32.9  | 0.16  | 99.6%                                  | $\lesssim 10^{-4}$                            |
| 4.10                               | 0.27                                      | 39.5   | 32.1  | 0.33  | 98.8%                                  | $\lesssim 10^{-4}$                            |
| Cedar-W<br>(N <sub>2</sub> @ 1.71) | 0.27                                      | 33.8   | 23.5  | 0.04  | 99.2%                                  | $\lesssim 10^{-4}$                            |

Table 1: Performance of each Cedar-H design. The kaon tagging condition is the time coincidence of photons detected in at least 5 sectors; similarly the pion misidentification is also for a coincidence of at least 5 sectors. For comparison, the values for the currently operated Cedar-W have also been included.

### 3 Proposed KTAG with Cedar-H at 3.8 bar

A pressure of 3.8 bar has been chosen for Cedar-H, which combines a well-behaved distribution of light at the diaphragm aperture, Fig 6, with excellent illumination of the PMT array, Fig 7. A further comparison of its performances with the current Cedar-W is given in table 2, where the numbers of 4- and 5-fold coincidences for 1,000 kaons and 10,000 pions are presented.

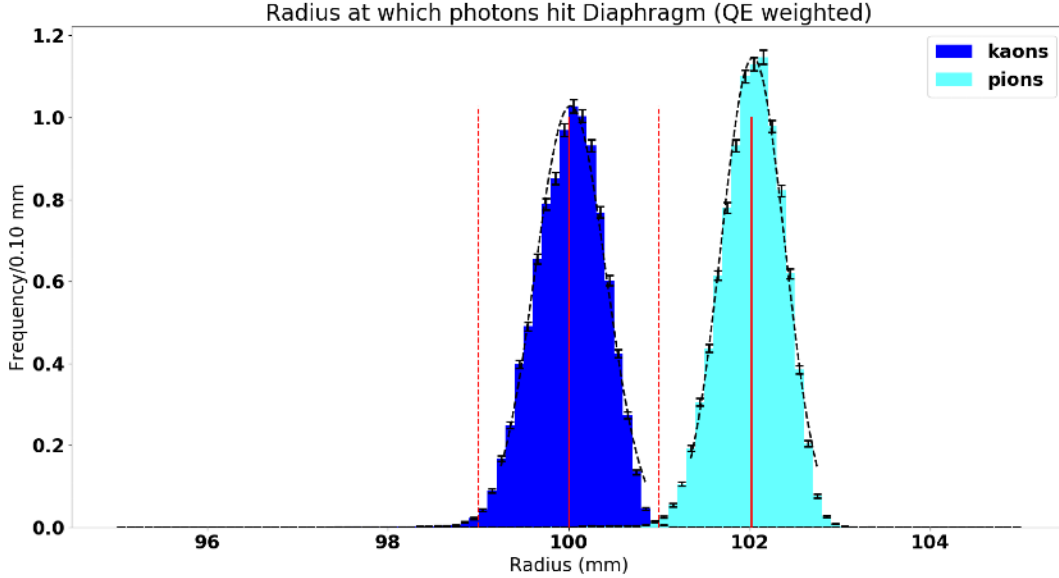


Figure 6: Light distribution at the diaphragm for the Cedar-H with radiator gas pressure of 3.80 bar. 1000 kaons (left) and 1000 pions (right) have been simulated. Quantum Efficiency (QE) of the PMTs has been applied.

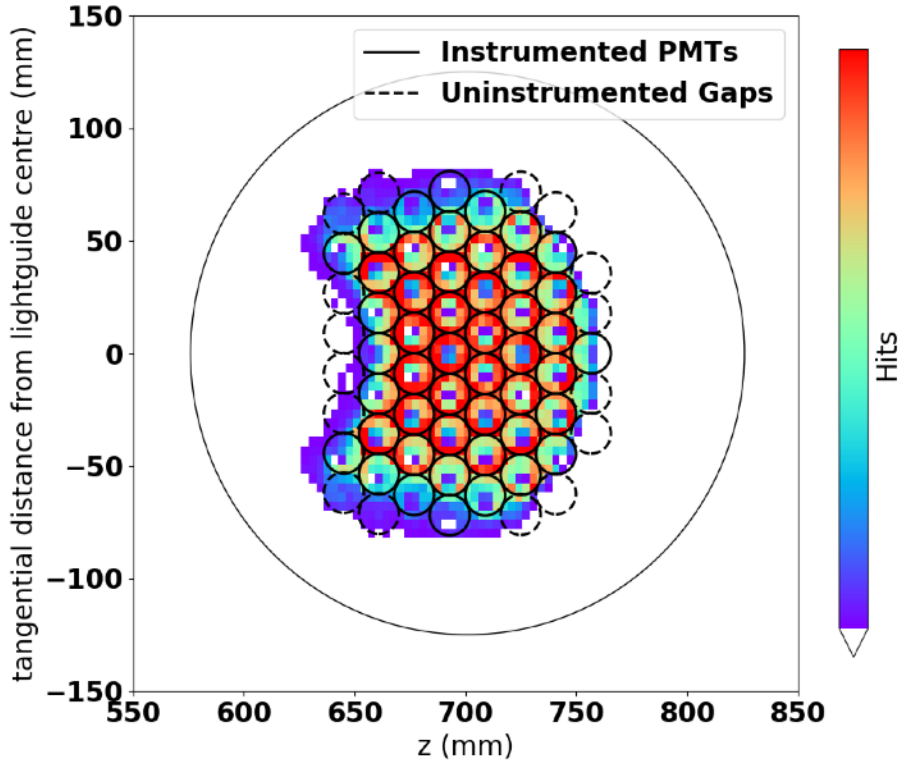


Figure 7: Distribution of light over the PMT array for a hydrogen radiator gas pressure of 3.80 bar. The circled areas indicate either an instrumented PMT (solid line) or uninstrumented gap (dashed line) where a PMT may be placed if this would be beneficial to the number of photons detected.

| CEDAR Design      | 1,000 Kaons      |                  | 10,000 Pions     |                  | Photons Per Pion At PMTs |
|-------------------|------------------|------------------|------------------|------------------|--------------------------|
|                   | $\geq 4$ Sectors | $\geq 5$ Sectors | $\geq 4$ Sectors | $\geq 5$ Sectors |                          |
| Cedar-H           | 995              | 995              | 3                | 0                | 0.11                     |
| Cedar-W ( $N_2$ ) | 993              | 992              | 2                | 0                | 0.04                     |

Table 2: Performance of KTAG for the new Cedar-H and current Cedar-W. Both designs show a high probability of identifying kaons with a low probability of detecting pions.

Due to the predicted 30% increase in photoelectrons compared with Cedar-W, the average hit rate in each PMT (labelled to match the KTAG MC handbook [5]) exceeds the maximum of 5MHz per channel that the read-out electronics can process. This is calculated assuming an average kaon rate of 50MHz (nominally 45MHz) and averaged over all eight sectors. Any additional photoelectrons, above the dashed line of Fig 8, will not be recorded and this will result in a loss of  $\sim 3$  photoelectrons per kaon assuming the same read-out. However, it is anticipated that new read-out electronics with a higher rate capability could be ready at the same time as the Cedar-H.

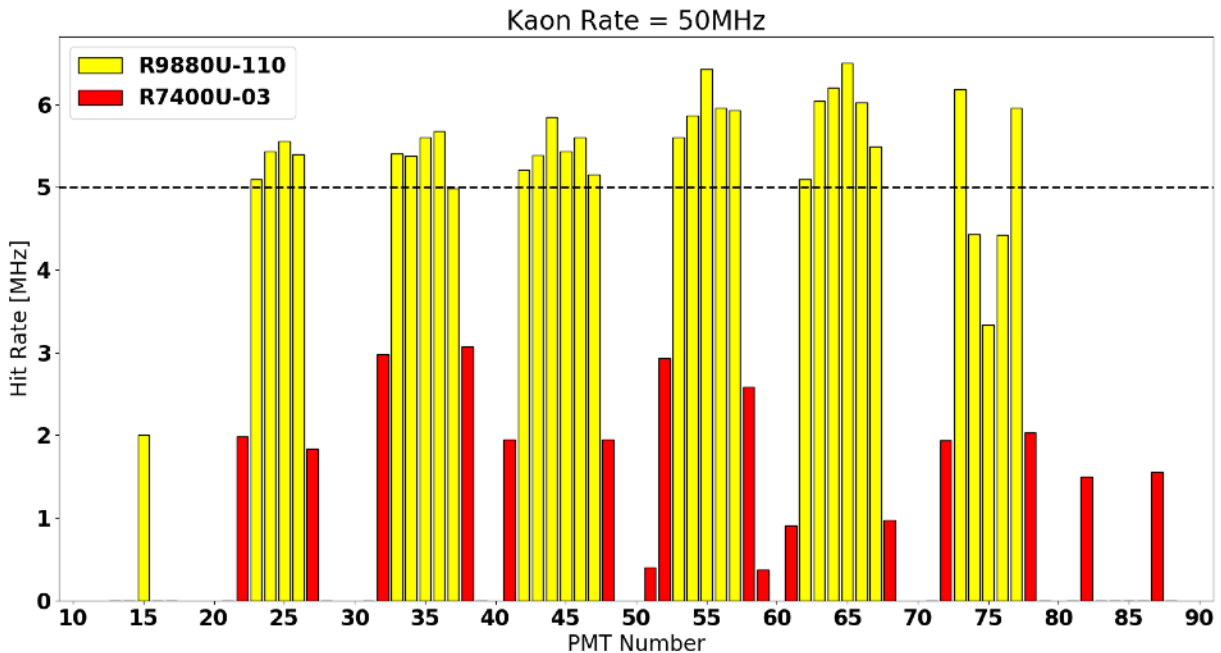


Figure 8: Average hit rate in each photomultiplier tube (PMT) for the new Cedar-H design assuming a kaon rate of 50MHz. The PMT numbers correspond to those found in the MC handbook [5]. Additionally, the colour of each bar represents the type of PMT used with those in yellow operating with a higher quantum efficiency than those in red. Current electronics allows for a maximum of 5MHz (dashed line) per channel with any additional information lost.

When calibrating Cedar the pressure must be adjusted to obtain the maximum kaon yield; for this to be successful the pion and kaon peaks must be separated. Fig 9a shows a simulated pressure scan (on a linear scale) displaying the pion and kaon peaks for a diaphragm aperture of width 1mm and perfect alignment of the detector with the beam. The kaon and pion peaks are clearly distinguishable. Such perfect alignment is unlikely to be achieved, however, and the effect of a misalignment of  $100\mu\text{rad}$ , comparable to the beam divergence of  $70\mu\text{rad}$ , is shown in Fig 9b. The separation between the kaon and pion peaks is lost for 4-fold coincidences, but reappears for 5- and 6-fold coincidences.

Table 3 summarises the parameters in the new Cedar-H design that have been modified from the current Cedar-W; a comprehensive list of KTAG parameters for each changed component is given in the appendix.

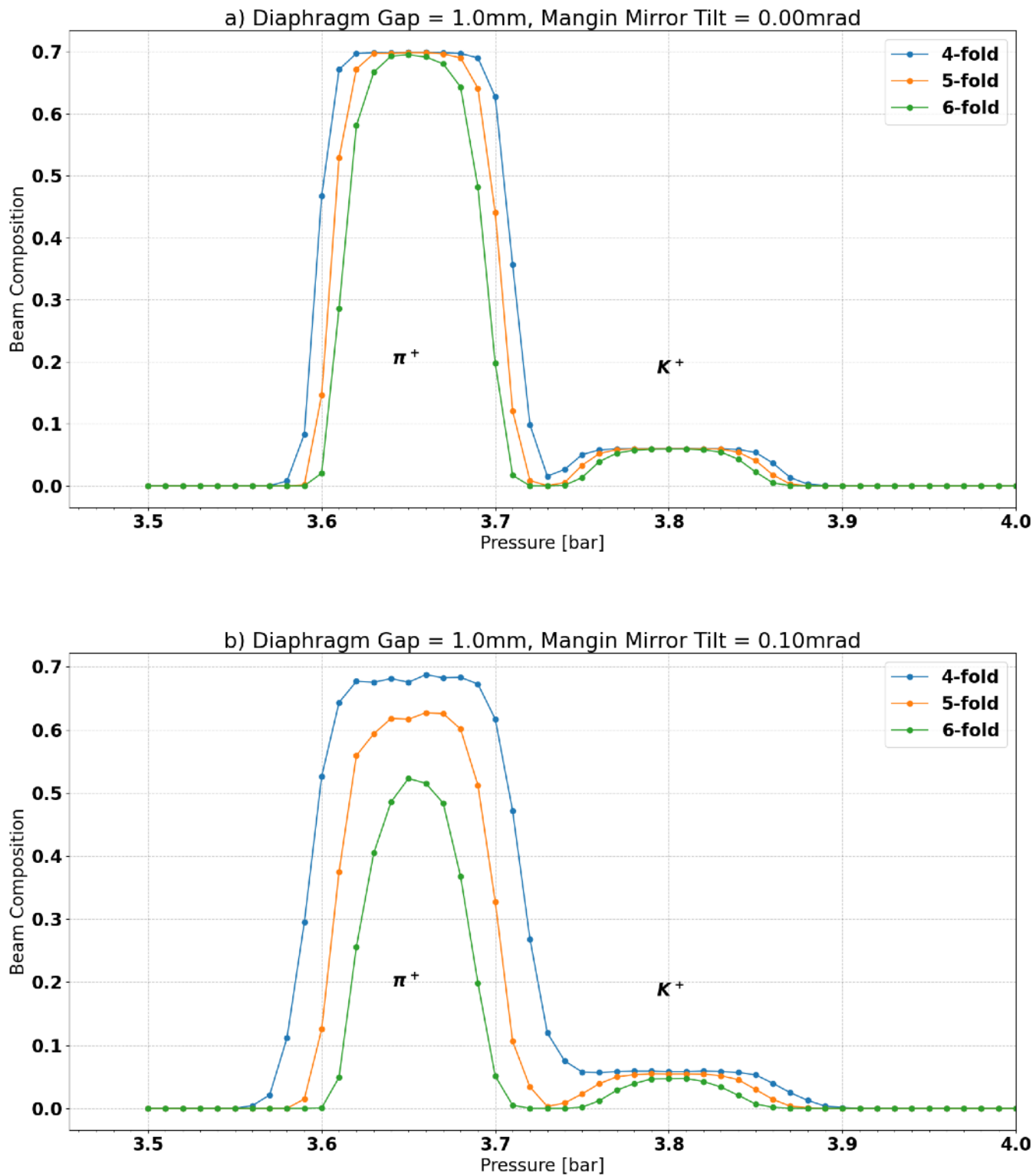


Figure 9: Pressure scans for the new Cedar-H design for a diaphragm aperture of 1mm. (a) Perfectly aligned Cedar; (b) Misalignment of the Mangin Mirror by 0.10mrad.

|  |            |
|--|------------|
| Pressure   | 3.80 bar   |
| <b>Cedar</b>   | Value [mm] |
| Mangin Mirror Reflective Surface Radius of Curvature | 9770       |
| Mangin Mirror Refractive Surface Radius of Curvature | 8994       |
| Chromatic Corrector Radius of Curvature              | 1307       |
| Mangin Mirror Inner Radius                           | 40         |
| <b>KTAG</b>  | Value [mm] |
| Spherical Mirror Surface Radius                      | 77.52      |
| Spherical Mirror Radial Offset                       | 106.0      |

Table 3: Required changes to the Cedar internal and external optics for the new Cedar-H design. All other parameters remain unchanged for Cedar-W and are reported in the appendix.

## 4 Tolerances on Optical and Mechanical Parameters

In order to build the new Cedar-H it is necessary to determine the tolerances on the radii of curvature of the three optical surfaces and location of their centres of curvature, together with the angles of tilt of the Mangin Mirror and Corrector Lens, so that the detector performs as expected. To calculate these tolerances, each parameter was individually varied and the number of photoelectrons at the PMTs calculated. A loss of 10% in the average number of detected photoelectrons per kaon was chosen as a measure of the tolerance on each parameter. There are three reasons why the loss may occur:

- Altering of the light ring radius at the diaphragm
- Broadening of the light ring
- Displacement/distortion of the light ring.

Of these, the changing radius can be accommodated by a change in the gas pressure, while the broadening of the light ring was found to be insignificant. Light losses resulting from a displacement of the ring cannot be recovered, and thus strict tolerances need to be found for the parameters that cause this. In general, any parameter that breaks the cylindrical symmetry of the Cedar will cause a displacement or distortion of the ring, and so the tolerances on the alignment of the lenses, together with the positions of their centres of curvatures, are likely to be critical.

Table 4 shows the required tolerances for building the Mangin Mirror and Chromatic Corrector for the new Cedar-H design along with their alignment in the Cedar vessel. It is important to note that the tilt of each lens is defined as the z distance between the outer radius of the lens and its nominal position. Additionally, the tolerance of non-uniformity in refractive index was assessed by randomly choosing a value of refractive index ( $n$ ) from a Gaussian distribution for each Cherenkov photon intersecting the lens. The tolerance is the RMS of the distribution that results in a 10% reduction in the detected number of photoelectrons. All parameters are straightforward for a manufacturer to achieve, but great care is required when aligning the Mangin Mirror inside the Cedar vessel as the tolerance is exceedingly small<sup>†</sup>.

---

<sup>†</sup>The alignment procedure for the Mangin Mirror is currently under study by physicists from the University of Birmingham and engineers from CERN.

|  | Value |
|--|-------|
| <b>Mangin Mirror</b>                                   |       |
| Radial Position of Lens [mm]:                          | 1.00  |
| Radius of Curvature (reflect) [mm]:                    | 50    |
| Radius of Curvature (refract) [mm]:                    | 100   |
| Radial Position of Centre of Curvature (reflect) [mm]: | 0.7   |
| Radial Position of Centre of Curvature (refract) [mm]: | 2.0   |
| Thickness [mm]:  | 5     |
| Tilt (dZ) [ $\mu\text{m}$ ]:                           | 15    |
| $\Delta n/n$   | 2%    |
| <b>Chromatic Corrector</b>                             |       |
| Radial Position of Lens [mm]:                          | 2.0   |
| Radius of Curvature [mm]:                              | 10    |
| Radial Position of Centre of Curvature [mm]:           | 1.7   |
| Thickness [mm]:  | 5     |
| Tilt (dZ) [mm]:  | 15    |
| $\Delta n/n$   | 0.1%  |
| <b>Spherical Mirror (KTAG)</b>                         |       |
| Radial Offset [mm]:                                    | 1.50  |
| z Position [mm]:                                       | 10.0  |

Table 4: Tolerances for building the new lenses and positioning of the spherical mirror.

## 5 Summary

A satisfactory design of a Cedar-H, using hydrogen at 3.8 bar as the Cherenkov radiator, has been developed and its performance shown to compare favourably with the current Cedar-W filled with nitrogen. The methodology employed has been shown to be robust, cross-checked with an independent study, and the tolerances on all parameters determined. Simulation of the pressure scan shows that the detector can be aligned with the beam. No significant problems in the manufacture or assembly of components is foreseen.

## References

- [1] F. Hahn *et al.*, NA62 Collaboration, *NA62: Technical Design Document*, NA62-10-07. (2010).
- [2] C. Bovet *et al.*, *The Cedar Counters for Particle Identification in the SPS Secondary Beams* DOI: 10.5170/CERN-1982-013. (1982).
- [3] E. Goudzovski *et al.*, *Development of the kaon tagging system for the NA62 experiment at CERN*, NIM **A801** (2015), pp. 86-94.
- [4] M. J. Riedl. *The mangin mirror and its primary aberrations*, doi: 10.1364/AO.13.001690. (1974).
- [5] NA62Twiki, <https://twiki.cern.ch/twiki/bin/viewauth/NA62/CedarDetector>.

## Appendix: Cedar Parameter Values

Table 5 shows the values of parameters used in the Cedar-H simulations (NA62FW) highlighting the difference between Cedar-W and Cedar-H. The origin of the coordinate system is the start of the old Cedar nose ( $z=69.278\text{m}$ ) and unless otherwise stated all values quoted are in mm.

|                     | Cedar Type<br>Gas<br>Pressure [bar] | Cedar-W<br>$\text{N}_2$<br>1.71 | Cedar-H<br>$\text{H}_2$<br>3.80 |
|---------------------|-------------------------------------|---------------------------------|---------------------------------|
| <b>Cedar</b>        |                                     |                                 |                                 |
| Front Vessel        | Length                              | 339.0                           | 280.0                           |
|                     | Inner Radius                        | 139.0                           | 139.0                           |
|                     | Outer Radius                        | 150.0                           | 150.0                           |
| Main Vessel         | Length                              | 4500.0                          | 4500.0                          |
|                     | Inner Radius                        | 267.0                           | 267.0                           |
|                     | Outer Radius                        | 279.0                           | 279.0                           |
| Chromatic Corrector | Z (upstream surface)                | 2234.0                          | 2281.0                          |
|                     | Radius Of Curvature                 | 1385.0                          | 1307.0                          |
|                     | Central Thickness                   | 20.0                            | 20.0                            |
|                     | Inner Radius                        | 75.0                            | 75.0                            |
|                     | Outer Radius                        | 160.0                           | 160.0                           |
| Mangin Mirror       | Z (upstream surface)                | 5732.0                          | 5741.0                          |
|                     | Radius Of Curvature (refracting)    | 6615.0                          | 8994.0                          |
|                     | Radius Of Curvature (reflecting)    | 8610.0                          | 9770.0                          |
|                     | Central Thickness                   | 40.0                            | 40.0                            |
|                     | Inner Radius                        | 50.0                            | 40.0                            |
|                     | Outer Radius                        | 150.0                           | 150.0                           |
| Diaphragm           | Z (centre)                          | 1251.0                          | 1290.0                          |
|                     | Radial Position Of Aperture         | 100.0                           | 100.0                           |
|                     | Aperture Diameter                   | 2.0                             | 2.0                             |
| Condensers          | Z (upstream surface)                | 1211.0                          | 1250.0                          |
|                     | Maximum Thickness                   | 10.0                            | 10.0                            |
|                     | Radius Of Curvature                 | 300.0                           | 300.0                           |
| Quartz Windows      | Z (upstream surface)                | 851.0                           | 910.0                           |
|                     | Thickness                           | 10.0                            | 10.0                            |
|                     | Radius                              | 22.5                            | 22.5                            |
|                     | Radial Offset (of centre)           | 103.0                           | 103.0                           |
| <b>KTAG</b>         |                                     |                                 |                                 |
| Spherical Mirrors   | Z (of cap centre)                   | 701.0                           | 701.0                           |
|                     | Radius Of Curvature                 | 51.68                           | 77.52                           |
|                     | Diameter                            | 50.0                            | 50.0                            |
|                     | Central Angle (deg)                 | 45.0                            | 45.0                            |
|                     | Radial Offset (of cap centre)       | 106.0                           | 106.0                           |

Table 5

## Appendix: Tolerance Plots

Mangin Mirror:



Figure 10

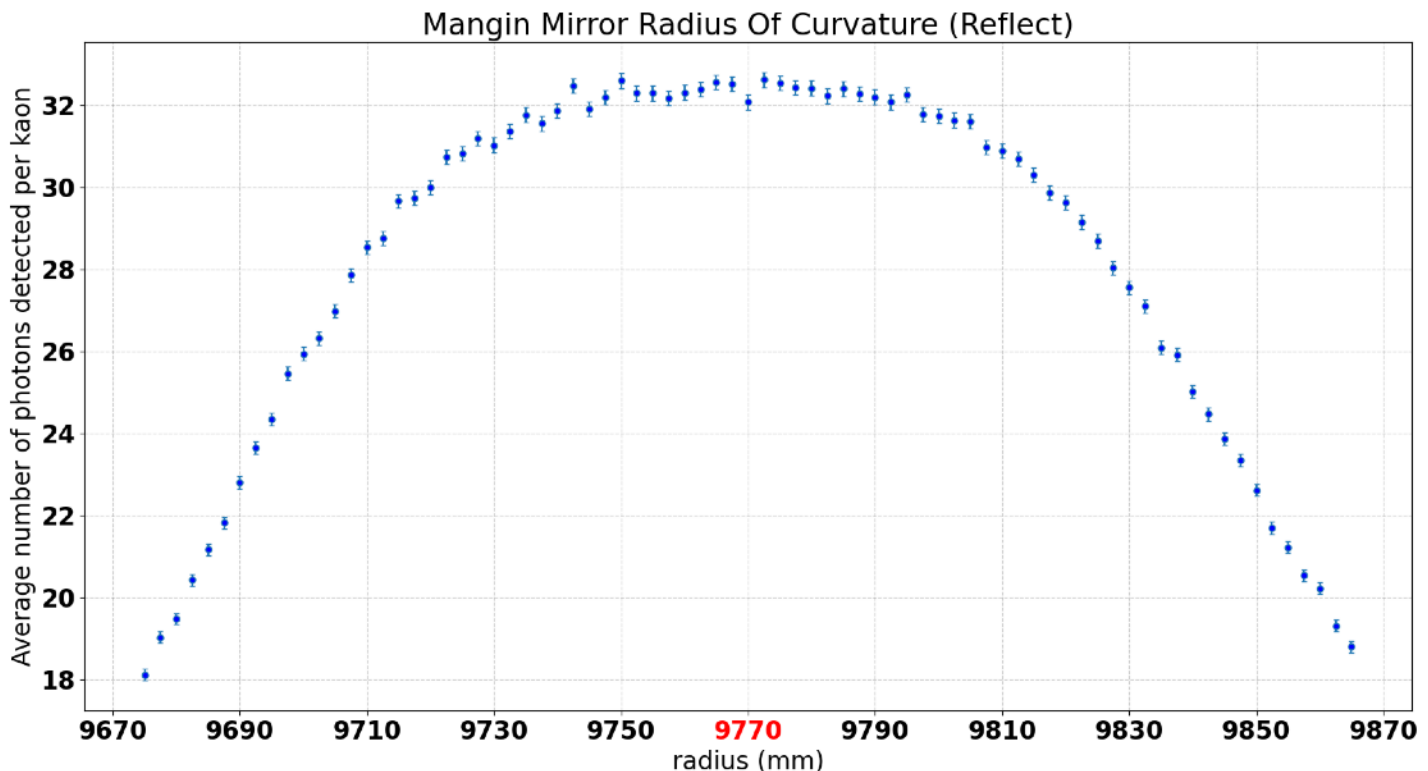


Figure 11

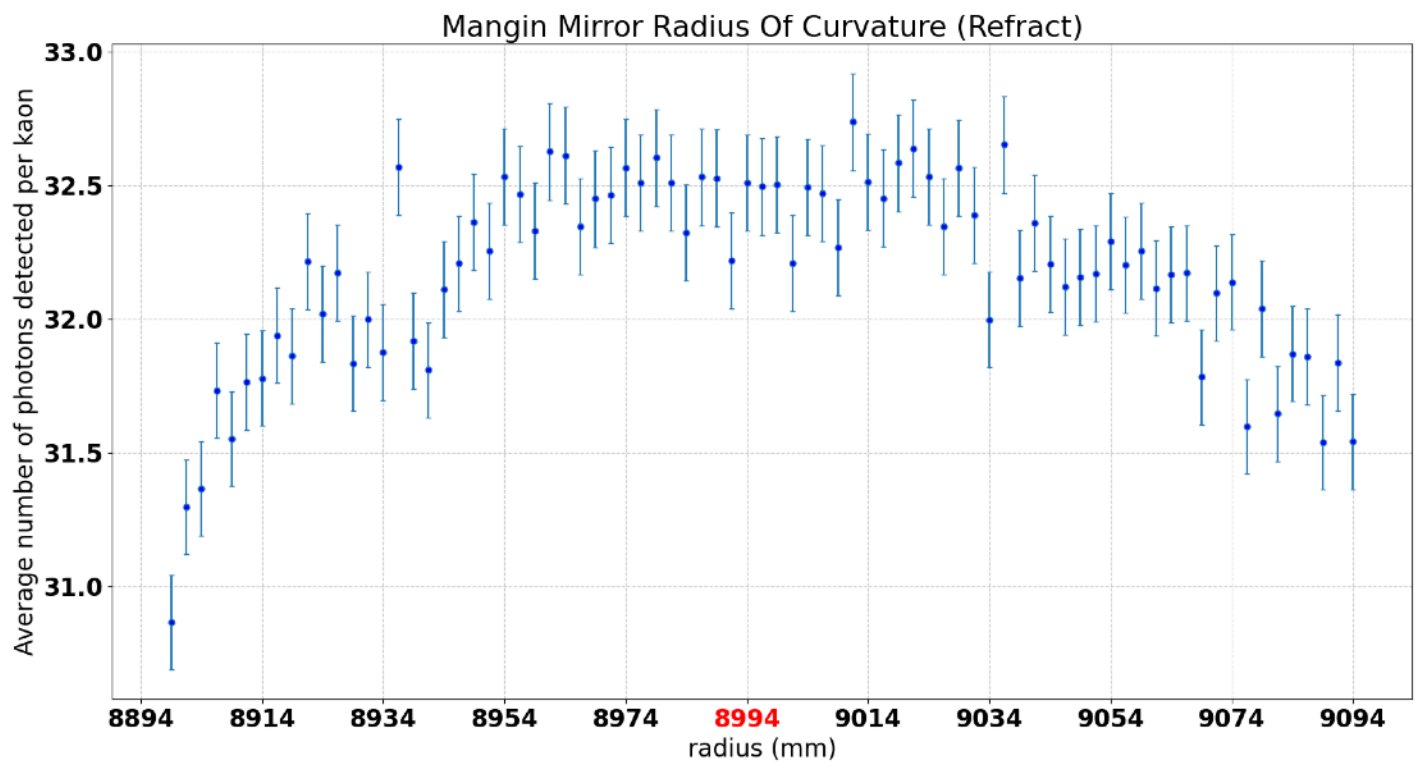


Figure 12

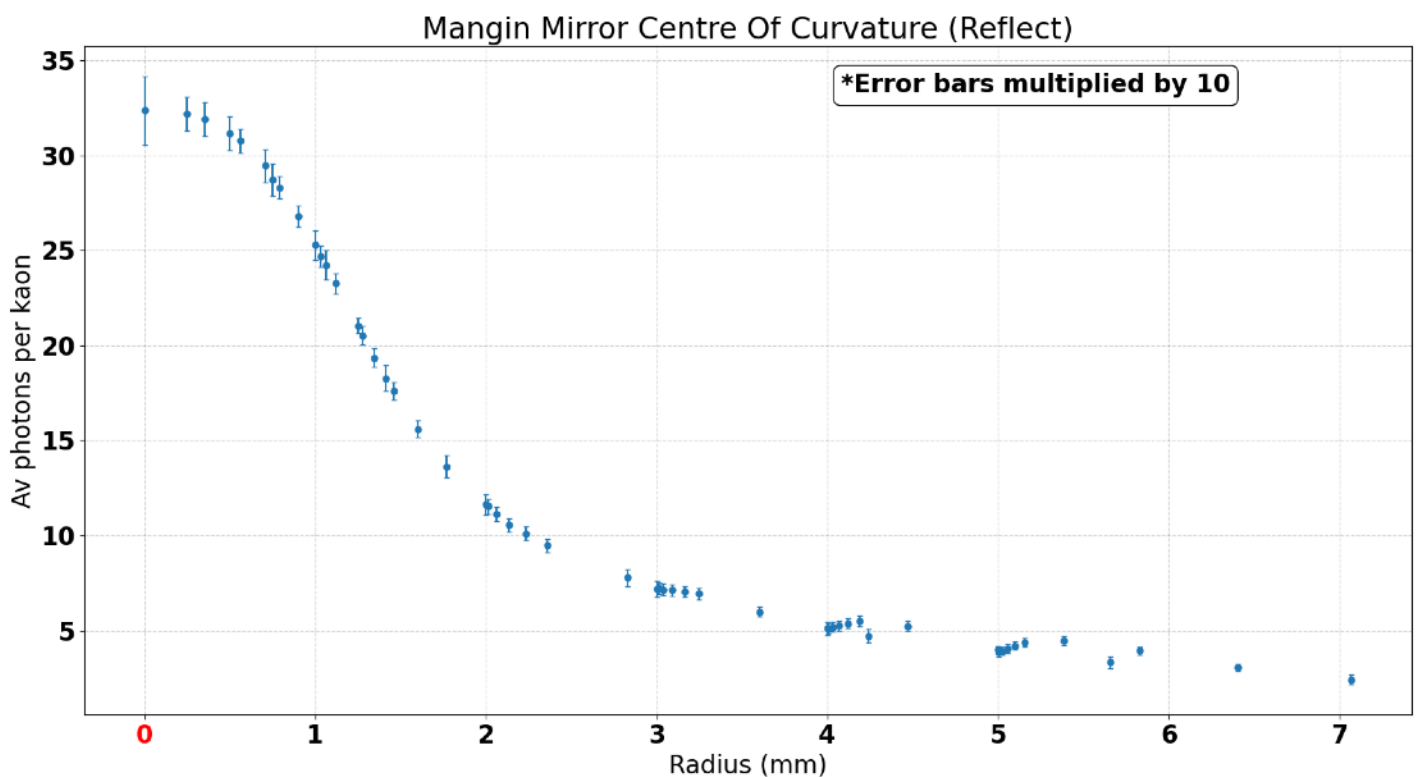


Figure 13

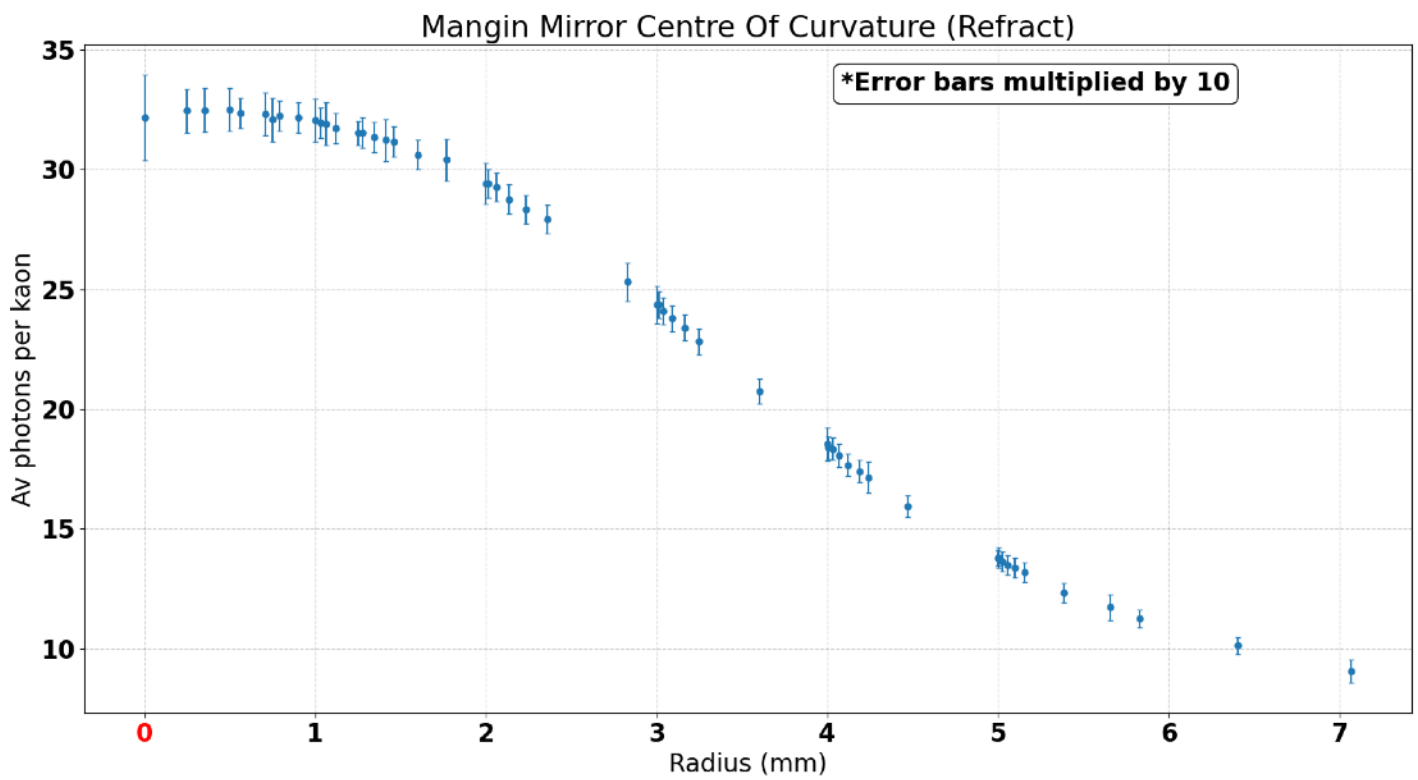


Figure 14

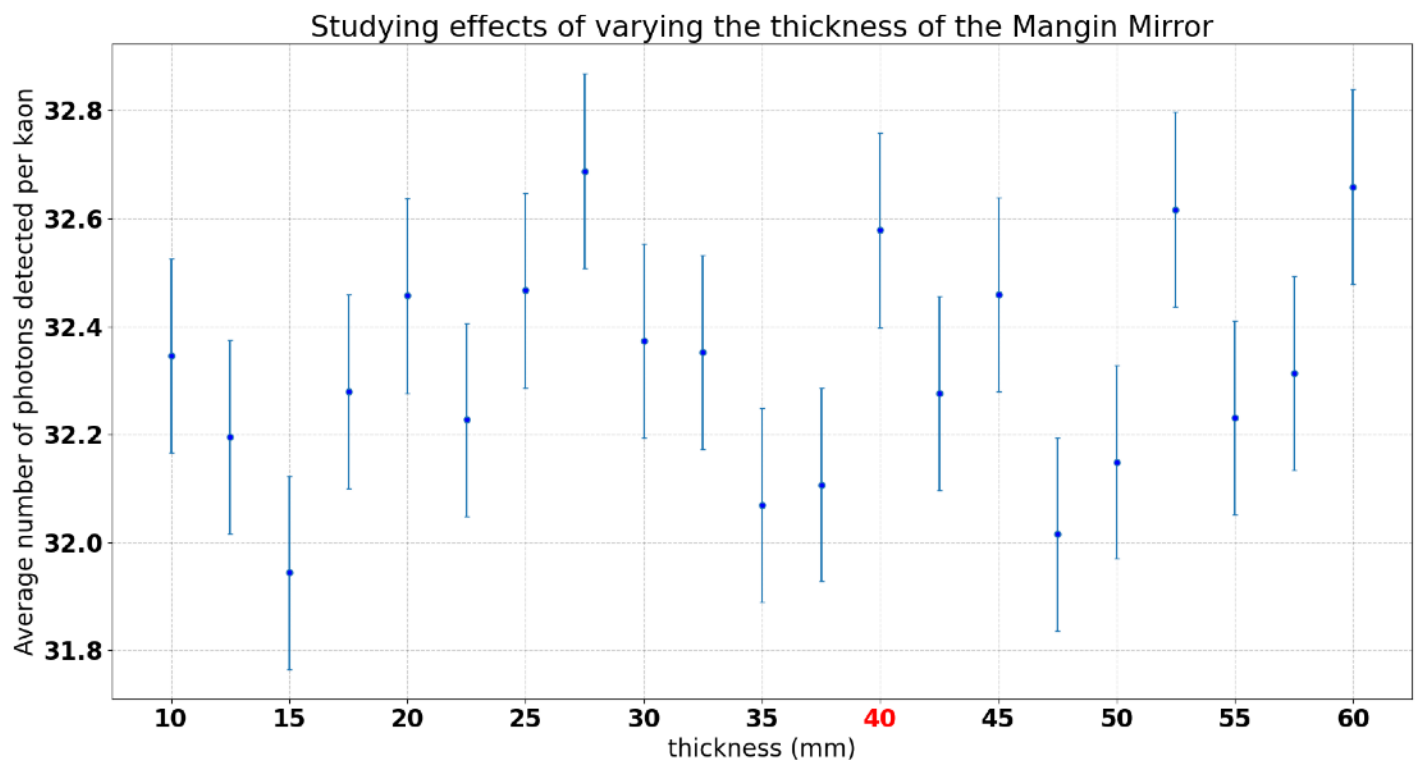


Figure 15

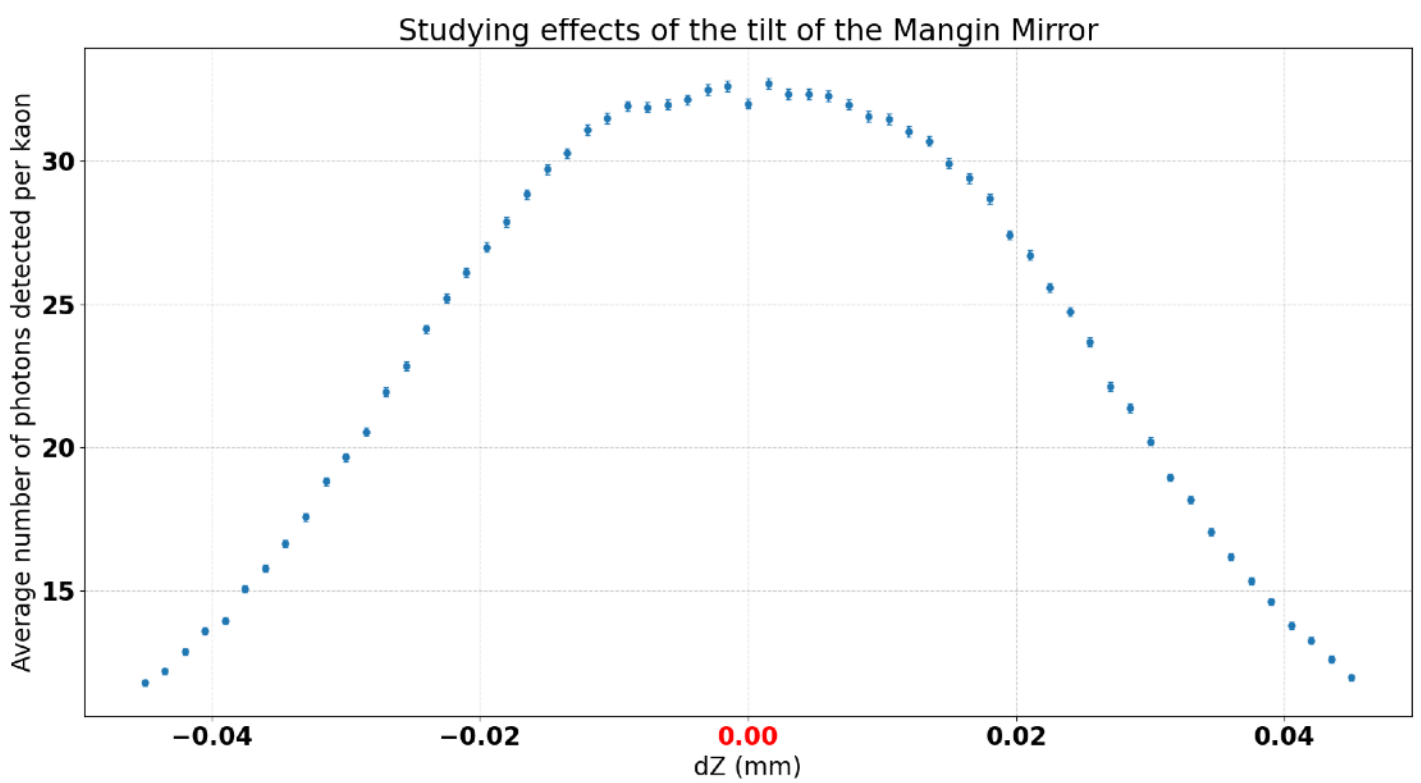


Figure 16

## Chromatic Corrector:

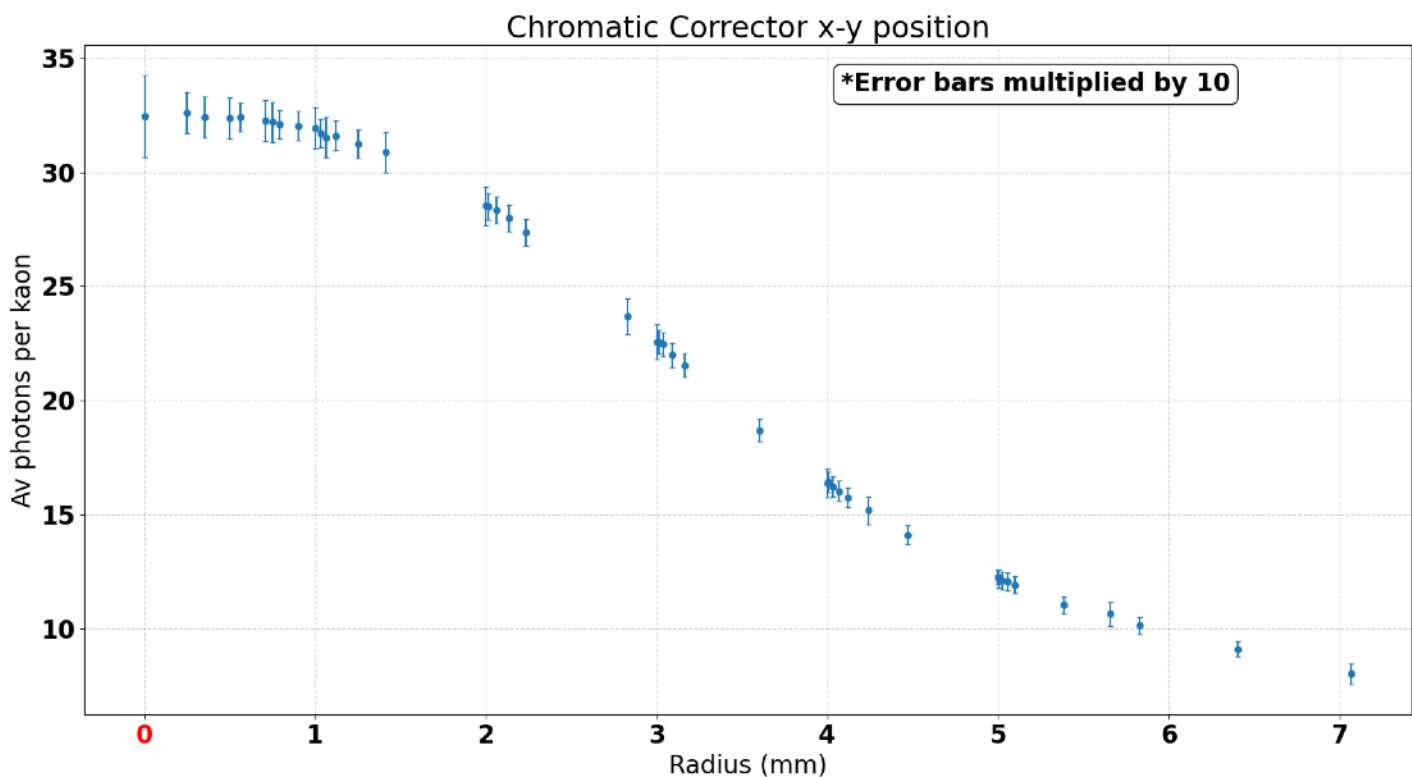


Figure 17

Studying the effects of altering the radius of curvature of the Chromatic Corrector

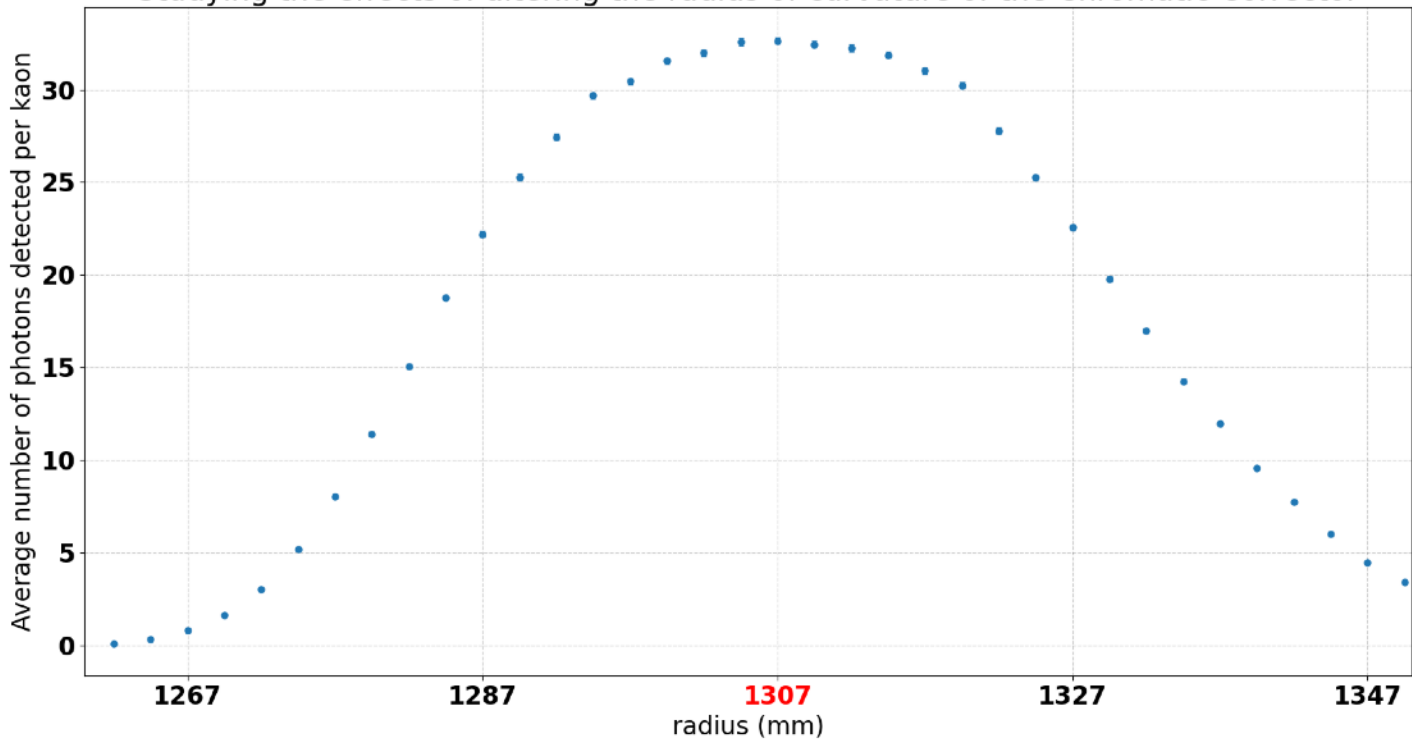


Figure 18

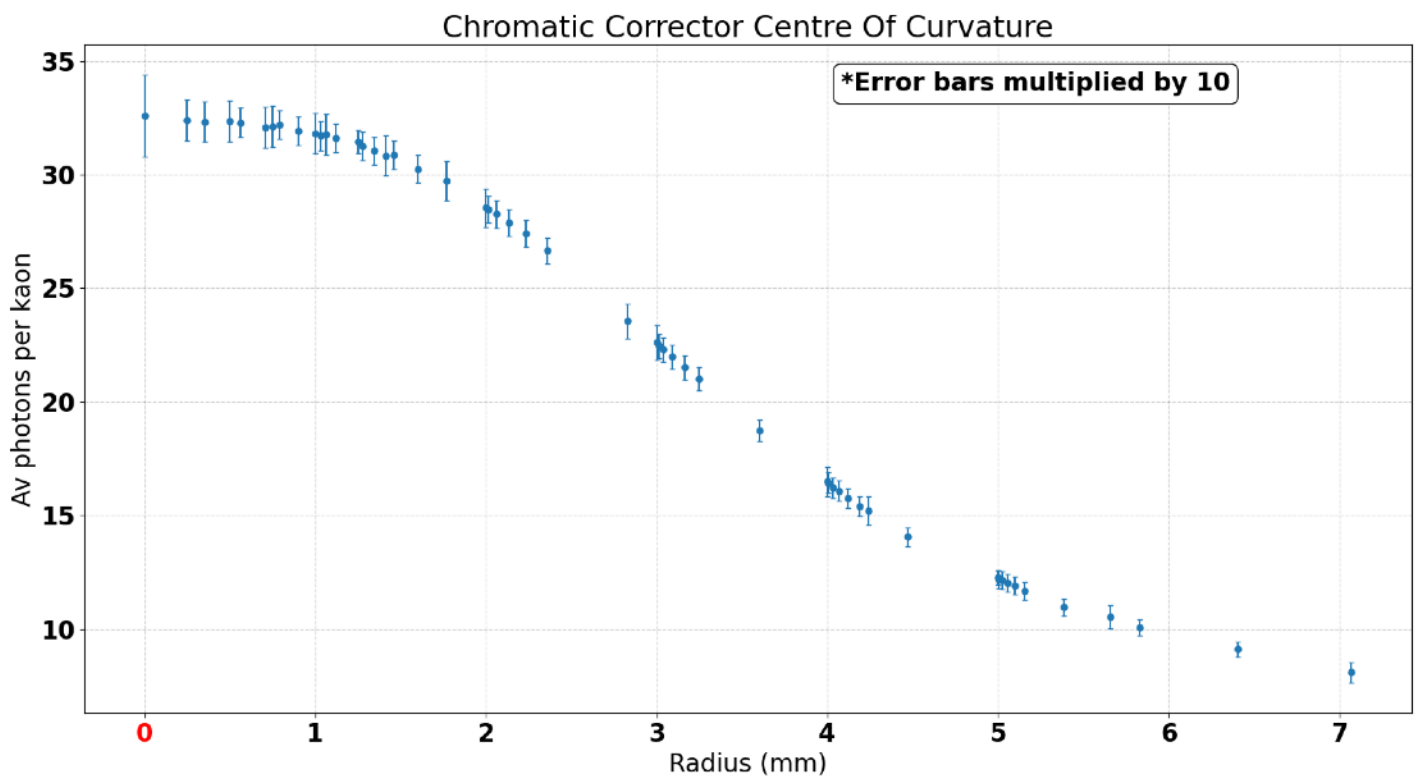


Figure 19

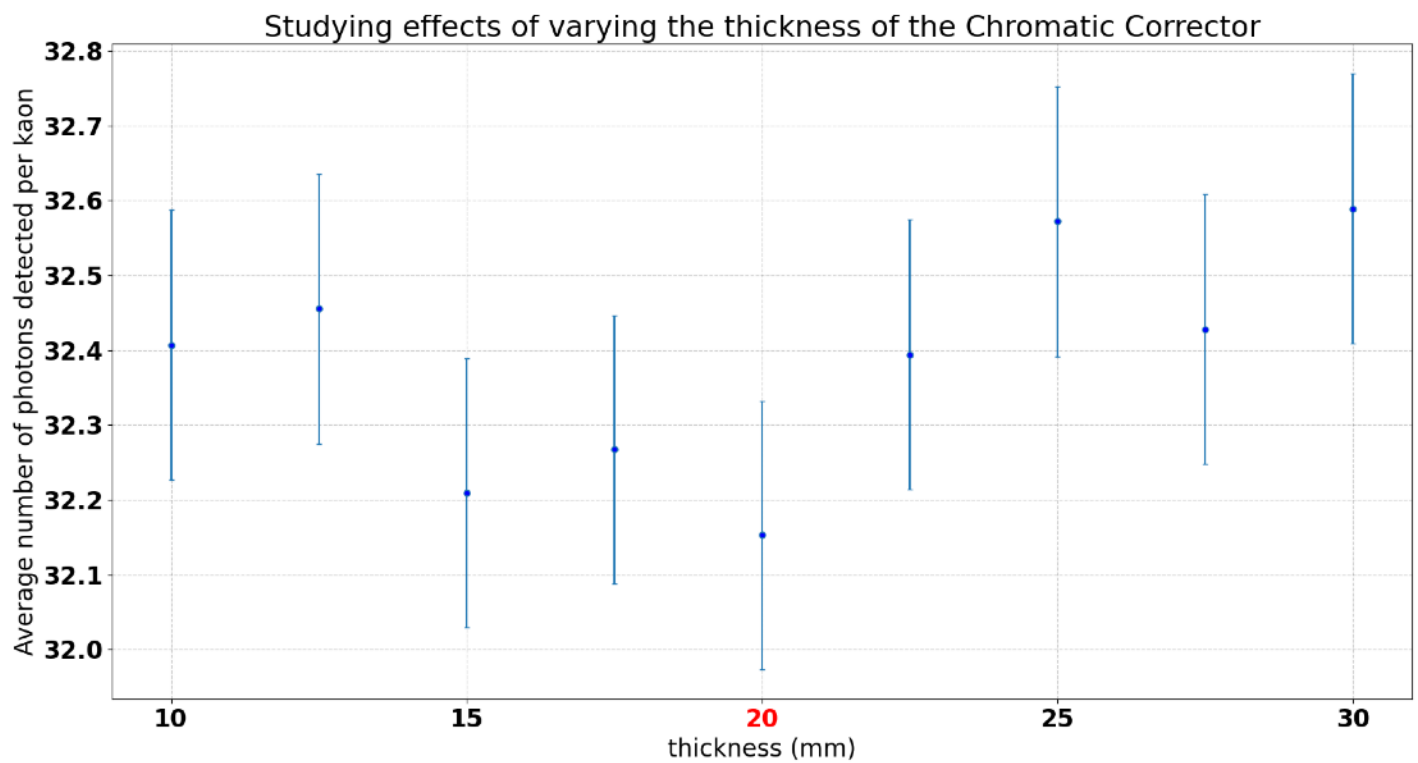


Figure 20

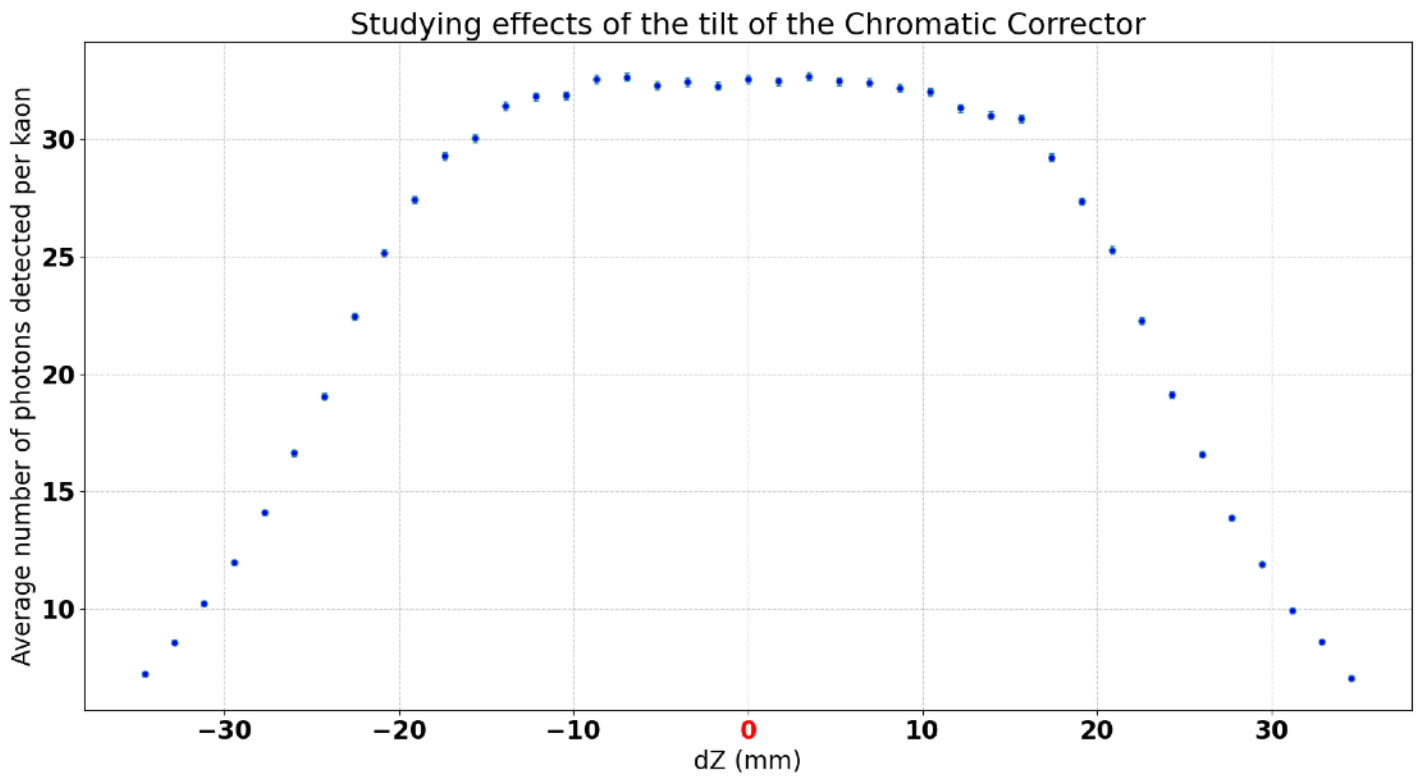


Figure 21

## Spherical Mirror:

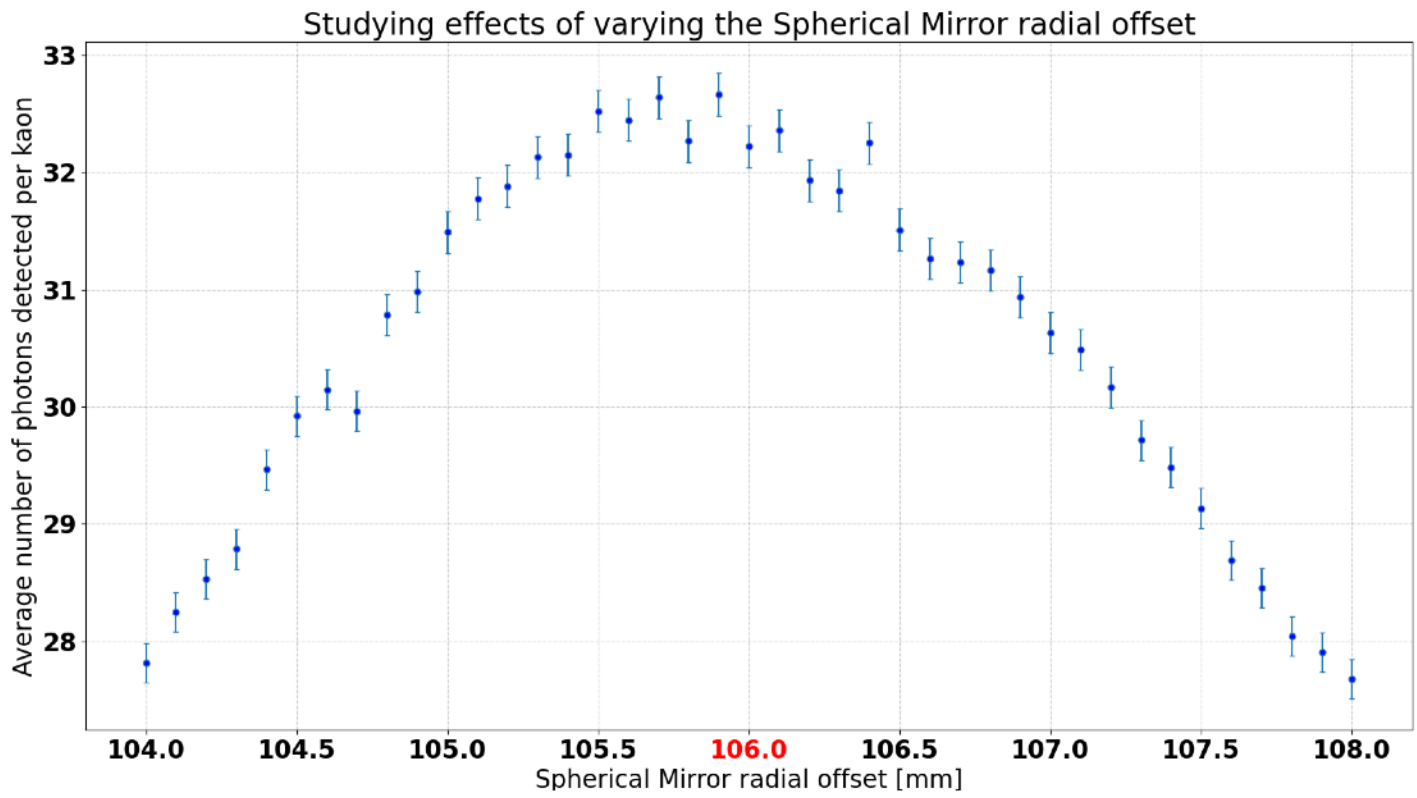


Figure 22

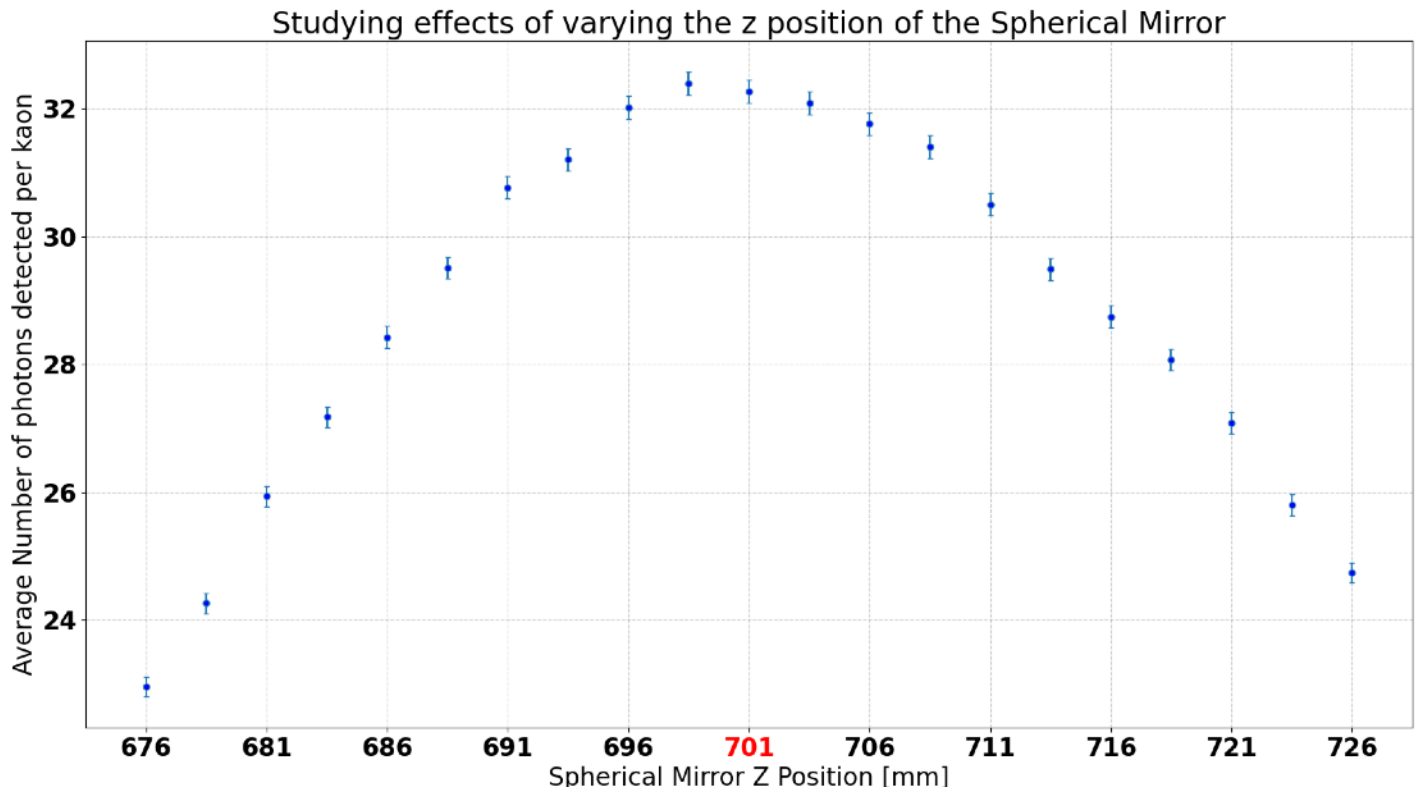


Figure 23